

Composition and fate of short-period super-Earths

The case of CoRoT-7b

D. Valencia¹, M. Ikoma^{1,2}, T. Guillot¹, and N. Nettelmann³

¹ Observatoire de la Côte d’Azur, Université de Nice-Sophia Antipolis, CNRS UMR 6202, BP 4229, F-06304 Nice Cedex 4, France

² Dept. of Earth and Planetary Sciences, Tokyo Institute of Technology, Ookayama, Meguro-ku, Tokyo 152-8551, Japan

³ Institut für Physik, Universität Rostock, D-18051 Rostock, Germany

Preprint online version: April 30, 2022

ABSTRACT

Context. The discovery of CoRoT-7b, a planet of radius $1.68 \pm 0.09 R_{\oplus}$ with an orbital period of 0.854 days demonstrates that small planets can orbit extremely close to their star.

Aims. Several questions arise concerning this planet, in particular concerning its possible composition, mass and fate.

Methods. We use knowledge of hot Jupiters, mass loss estimates and models for the interior structure and evolution of planets to understand its composition, structure and evolution.

Results. Although detailed modeling should address this problem, we show that a relatively significant mass loss $\sim 10^{11} \text{ g s}^{-1}$ is to be expected, independently of the planet’s composition. Given the closeness to the star, we find that the planet size is compatible with the observations only if the planet contains less than 1% of its mass in hydrogen and helium and less than 20% in steam. Due to the significant evaporation rate, it is most likely that the planet is made only of iron and silicates, which implies that its mass should be in the range 4 to $15 M_{\oplus}$. However the origin of CoRoT-7b is unknown: It may have always had a terrestrial composition, it may be the remnant of a Uranus-like ice giant, or a gas giant with a small core that would have been entirely stripped of its gaseous envelope.

Conclusions. Our predictions can be tested by measurements of the planet mass and possibly by the detection of evaporating silicates, with a rate that should be within an order of magnitude that measured for HD209458b.

1. Introduction

The newest planet discovered by space mission CoRoT is remarkably interesting. CoRoT-7b is not only the first super-Earth with a measured radius, but orbits extremely close to its parent star, only 4.27 stellar radii away (Leger et al., 2009). While its radius was measured from CoRoT lightcurves, its mass is still to be confirmed from detailed analyses of radial-velocity observations, and hence its composition remains undetermined. Even with precise mass (M) and radius (R) measurements, the composition of a planet will remain ambiguous (Valencia et al., 2007b; Adams et al., 2008). This is the case because different combinations of the compositional end members (silicate mantles, iron cores, H_2O , and H/He in the cases of massive super-Earths) can share the same M and R . However, this data is enough to establish if the planet is too large to be terrestrial (its radius is larger than the maximum size of a coreless silicate planet), or too large to be icy or terrestrial (its radius is larger than the maximum size of a snowball planet) for its mass. In this study we use this information, in combination with structure models and atmospheric evaporation scenarios to investigate the physical nature of CoRoT-7b. The framework presented here is applicable to any transiting close-in super-Earth. Moreover, owing to the bias of discovering short-period planets, we expect many such super-Earths to be discovered in the near future with the next phases of CoRoT and Kepler’s observations.

The radius and orbital period of CoRoT-7b are $R = 1.68 \pm 0.09 R_{\oplus}$ and $P = 0.854$ days respectively, and the calculated age and equilibrium temperature are $\sim 1.2 - 2.3$ Gyr and $1800 - 2600$ K (Leger et al., 2009), respectively. Under such conditions, we first consider the fate of an atmosphere (section 2). After a description of the model used to calculate the planet’s structure (section 3), we present general results (section 4) for close-in super-Earths composed of refractory material – silicates and/or iron – including evaporation scenarios for the silicate portion, as well as planets with a substantial amount of ices. We discuss its possible evolution as an evaporated ice or gas giant planet and limit its maximal present amount of steam or H/He (section 4). We conclude by providing arguments for the most likely scenario for CoRoT-7b.

2. Mass Loss

Close-in planets are vulnerable to evaporation because of intense irradiation from their parent star. Indeed, gas has been detected to flow out from transiting gas giant HD 209458b (Vidal-Madjar et al., 2003). Certainly, CoRoT-7b, whose mean density is $3-12 \text{ g cm}^{-3}$ (a likely mass between 4 and $11 M_{\oplus}$ being assumed) is denser than HD 209458b ($\bar{\rho} = 0.33 \text{ g cm}^{-3}$) by at least an order of magnitude. However, the UV flux received by CoRoT-7b is greater by an order of magnitude, because it is closer to its parent star (0.017 AU) and somewhat younger compared to

HD209458b (0.047 AU and ~ 4 Gyr). One could therefore expect mass loss rates that are comparable within an order of magnitude for the two planets. Consequently, given that CoRoT-7b is 20 to 55 times less massive than HD 209458b, this mass loss may have a profound effect on its evolution, fate and present composition. We now attempt to quantify this mass loss, using simple assumptions (the precise modelling of atmospheric escape in this planet is a difficult task beyond the scope of this article).

We model the atmospheric escape using the well-known expression for the extreme case of energy-limited escape, the validity of which has been verified for gas-giant planets close to their star (see review by Yelle et al., 2008):

$$\dot{M}_{\text{esc}} = \frac{3\epsilon F_{\text{xuv}}}{G\bar{\rho}_p K_{\text{tide}}}, \quad (1)$$

where F_{xuv} is the incident flux of the stellar EUV (extreme ultraviolet radiation), ϵ is the heating efficiency defined as the ratio of the net heating rate to the rate of stellar energy absorption, $\bar{\rho}_p$ is the mean density of the planet, K_{tide} is a correction factor to include the Roche-lobe effect (Erkaev et al., 2007; Lecavelier des Etangs et al., 2004), and G is Newton's constant. Of course, most of the physics is hidden in the parameter ϵ which is mainly controlled by the ability of the upper atmosphere to cool. In the case of close-in gas giants, detailed calculations show that H_3^+ plays a dominant role for the cooling of the upper atmosphere. In particular, Eq. (1) with $\epsilon = 0.1$ and HD 209458b's characteristic values yields $\dot{M}_{\text{esc}} = 4 \times 10^{10} \text{ g s}^{-1}$, which is to be compared to values between 3.5 and $4.8 \times 10^{10} \text{ g s}^{-1}$ obtained in the literature (Yelle et al., 2008, and references therein).

For planets with different atmospheric compositions, one may question the validity of the relation. Tian et al. (2008) have recently simulated the escape of the Earth's atmosphere for different EUV irradiation levels. They demonstrate that, for EUV irradiation fluxes above ~ 10 times the solar value, the atmosphere is in the hydrodynamic regime, namely that it escapes in an energy-limited fashion rather than through blow-off or in a diffusion-limited way. While thermal conduction is important for moderate EUV fluxes, implying that mass loss then depends on atmospheric composition, its contribution is found to become negligible for strong EUV fluxes –as it is in our case–. This can also be seen by the fact that the ratio of the EUV flux that the planet receives to a typical energy flux due to thermal conduction is $\beta \approx 10^{10-11}$, and that the ratio of a typical energy flux to a thermal conduction flux is $\zeta \approx 10^{3-5}$, provided that the thermal conduction coefficient is of the same order of magnitude as that for hydrogen molecules (see García Muñoz (2007), for a similar discussion about HD209458 b, and Watson et al. (1981) for a precise definition of β and ζ).

As described above, the escape efficiency is controlled by the radiative cooling by H_3^+ in the case of hydrogen atmospheres. In the case of water-rich atmospheres, oxygen from dissociation of H_2O prevents a significant amount of H_3^+ from forming, which means the efficiency might be higher (e.g., García Muñoz, 2007). Indeed, from the values of the exobase temperature and velocity of Fig. 8 of Tian et al. (2008), one obtains the mass loss rate of the order of 10^9 g/s in the case of the highest EUV flux ($= 100 \text{ erg s}^{-1} \text{ cm}^{-2}$), while Eq. (1) yields a value of $\sim 10^9 \epsilon \text{ g/s}$. For silicate atmospheres, no calculations exist, but we can presume that in

the likely absence of species that cool much more efficiently than H_3^+ , Eq. (1) with $\epsilon = 0.1$ should remain valid within an order of magnitude –we will come back to this particular case in §4.1.3. In conclusion, *mass loss should remain relatively large whatever the properties of the atmosphere (and its mean molecular weight)*.

Another important quantity controlling the escape flux is the flux of EUV photons emitted by the star, which is strongly dependent on the stellar age:

$$F_{\text{xuv}} = \alpha t_9^{-\beta} a_1^{-2}, \quad (2)$$

according to recent observations of EUV emission from young stars (Ribas et al., 2005); where t_9 is the stellar age in Gyr, a_1 the planet's orbital distance in AU, and α and β are constants. Their best-fit result is obtained with $\alpha = 29.7 \text{ erg s}^{-1} \text{ cm}^{-2}$ ($\equiv \alpha_{\text{R05}}$) and $\beta = 1.23$. With this expression and values, one obtains that $F_{\text{xuv}} = 5.0 \times 10^4 \text{ erg s}^{-1} \text{ cm}^{-2}$ for CoRoT-7b ($t_9 = 1.8$ and $a_1 = 0.017$), while $2.4 \times 10^3 \text{ erg s}^{-1} \text{ cm}^{-2}$ for HD209458 b ($t_9 = 4.0$ and $a_1 = 0.047$).

Using values characteristic of CoRoT-7b in Eq. (1), one obtains

$$\dot{M}_{\text{esc}} = 1 \times 10^{11} t_9^{-\beta} f_{\text{esc}} \text{ g s}^{-1} \quad (3)$$

with

$$f_{\text{esc}} = \left(\frac{\alpha}{\alpha_{\text{R05}}} \right) \left(\frac{a_1}{0.017} \right)^{-2} \left(\frac{\epsilon}{0.1} \right) \left(\frac{\bar{\rho}_p}{\bar{\rho}_{\oplus}} \right)^{-1} \left(\frac{K_{\text{tide}}}{0.65} \right)^{-1}. \quad (4)$$

With the reported age of CoRoT-7b, $t_9 = 1.2\text{--}2.3$ (Leger et al., 2009), and $\beta = 1.23$, Eq. (3) yields values for the escape rate, $\dot{M}_{\text{esc}} = (5\text{--}10) \times 10^{10} \text{ g s}^{-1}$, similar to that for HD209458 b.

To obtain the total mass lost before t_9 , we integrate eq. (1), so that

$$M_{\text{esc}} = 0.7 \left(\frac{t_9^{1-\beta} - t_{9,0}^{1-\beta}}{1-\beta} + t_{9,0}^{1-\beta} \right) f_{\text{esc}} M_{\oplus}, \quad (5)$$

where $t_{9,0}$ is the time during which the EUV flux is constant and taken to be 0.1. Using eq.(5) with $\epsilon = 0.1$, assuming a planet density that is constant in time and CoRoT-7b's characteristic values, one obtains a cumulative escaped mass that goes from $\sim 1.5 M_{\oplus}$ for a $11 M_{\oplus}$ planet to $\sim 7 M_{\oplus}$ for a $3 M_{\oplus}$ planet. Hence if CoRoT-7b's present mass is less than $\sim 4 M_{\oplus}$, this would imply that it may have lost more than half of its initial mass, a case that is less likely. (With a strong caveat however: this assumes ϵ is close to 0.1).

Without a detailed calculation of heating and cooling effects which depend on the exact composition of the escaping atmosphere, this should be considered only as an order of magnitude estimate. However, it shows that for any atmosphere to be present, it must constantly be resupplied and that the planet may have already lost a significant fraction of its mass. On the other hand, this does not mean that this planet happened to be detected on its way to complete evaporation. By integrating eq. (3), one finds that the current state is rather stable; complete evaporation takes more than 10 Gyr for $\epsilon = 0.1$ and over 1 Gyr even for $\epsilon = 1$. In any case, our estimates leave room for a rather large ensemble of possibilities concerning the global composition of the planet: it may possess iron and rocks, but also ice (if

the planet formed at large distances and migrated inward), and the question of how much atmosphere (as steam or hydrogen and helium) may be present arises. We attempt to address this in the following sections.

3. Modelling interior structure and evolution

3.1. Procedure

In order to calculate the possible structure and evolution of Earth-like planets up to ice giants and gas giants, we combine two models. For the solid/liquid regions we use a 3 layer (iron/rock/ice) hydrostatic model based on Vinet and shock equations of states; each layer is assumed to be isentropic except for the conductive thermal boundary layers at the top and bottom of the mantle (Valencia et al., 2006, 2007b). This model reproduces the Earth’s structure well and has been used previously to understand super-Earths properties. For gaseous/fluid envelopes, we use a quasi-static model of interior structure and evolution that has been extensively used to model solar and extrasolar giant planets (Guillot & Morel, 1995; Guillot, 2005). The two models are tied by using the pressure at the bottom of the gaseous/fluid envelope as an upper boundary condition for the calculation of the structure of the solid/liquid interior. The temperature is *not* consistently calculated between the two models. However, this should not affect the results because thermal effects have a negligible impact on the properties of high-pressure iron, rocks and solid ices.

Our purpose is to understand possible compositions of CoRoT-7b. The thermal evolution of such a planet is uncertain because it depends on its composition, initial state, dynamical evolution, all of which are unknown. It also depends on atmospheric properties and opacities, two quantities that are difficult to estimate for a planet that probably has a very different atmospheric composition from what has been usually considered. Evolution calculations are therefore obtained using a simplified atmospheric boundary condition

$$T_{10} = T^* (1 + L/L_{\text{eq}})^{1/4}, \quad (6)$$

where T_{10} is the temperature at the 10 bar level, L is the planet’s intrinsic luminosity, L_{eq} corresponds to the stellar luminosity that it receives and T^* is chosen equal to 2500 K to account for the presence of a greenhouse effect similar to what is obtained for the atmospheres of close-in giant exoplanets (e.g. Iro et al., 2005). In fact, because the thermal evolution of highly irradiated planets is rapidly governed by the growth of an inner radiative zone, it is weakly dependent on the choice of the outer boundary condition. What is most important to us is that the high (~ 2000 K) irradiation temperatures of CoRoT-7b maintain the atmosphere well above the condensation temperature of water, so that a steam atmosphere may be present for a long time. (This is contrary to planets in colder environments which require a large L to maintain photospheric water vapor, and therefore cool quickly).

For opacities in gaseous envelopes, we use the Rosseland opacity table of Alexander & Ferguson (1994). The table is valid for a hydrogen-helium solar composition mixture so that its application to other atmospheres (e.g. one mainly formed with water vapor) may be questioned. We point out however that the cooling is generally controlled by the

opacity in a region at a pressure $P \sim 1 - 10$ kbar and $T \sim 3000$ K, for which the opacities are extremely uncertain, regardless of the assumed composition (Guillot et al., 1994). At these pressures and temperatures, it is mostly controlled by collision-induced absorption by molecules in the infrared, and by the presence of electrons that yield important absorption (e.g. from H^- for a hydrogen rich gas) at visible wavelengths. As a result, the opacities increase rapidly with increasing P and T , whatever the assumed composition. The switch from an almost isothermal external layer to a nearly adiabatic envelope in deeper regions is expected to occur abruptly. In this case also, the quantitative uncertainties on the underlying physical parameters are large, but they have a limited impact on the result, and they do not change qualitatively our conclusions.

Finally, the boundary condition at the bottom of the envelope is defined as a radius provided by the hydrostatic model of the solid/liquid interior, and a luminosity:

$$L_0 = \dot{\epsilon}_{\text{radioactive}} M_{\text{R}} + C_V \frac{dT_{\text{Fe+R}}}{dt} M_{\text{Fe+R}}, \quad (7)$$

where $\dot{\epsilon}_{\text{radioactive}}$ is the radioactive luminosity per unit mass, M_{R} is the mass of the (rocky) mantle, C_V is the rock + iron core specific heat, and $T_{\text{Fe+R}}$ is a characteristic temperature of the core of mass $M_{\text{Fe+R}}$. In the calculations, we assume a chondritic value $\dot{\epsilon}_{\text{radioactive}} = 2 \times 10^{20} \text{ erg s}^{-1} M_{\oplus}^{-1}$, $C_V = 10^7 \text{ erg g}^{-1} \text{ K}^{-1}$ and $dT_{\text{Fe+R}}/dt = dT_{\text{env}}/dt$, where T_{env} is the temperature at the bottom of the envelope. However, we found results to be quite insensitive to the choice of the inner boundary condition because for most cases, L was found to be significantly larger than L_0 .

3.2. States of matter inside CoRoT-7b

We now turn to investigate the different phases and states of matter for CoRoT-7b given the possible compositions.

3.2.1. Hydrogen and helium

In Uranus and Neptune, hydrogen and helium form about 1 to 4 M_{\oplus} of the planets’ outer envelopes (e.g. Guillot, 2005, and references therein). While it is not necessary expected in a planet as small in size as CoRoT-7b, it is interesting to consider them and provide upper limits to their abundances in the planet.

Of course, given the temperatures to be considered (~ 2000 K and above) and pressures well below a Mbar, hydrogen and helium are expected to behave as a gas with hydrogen in molecular form (see phase diagram in Guillot, 2005). The equation of state considered for modeling their behavior is that of Saumon et al. (1995).

3.2.2. Water and “ices”

With an effective average temperature of 1800 K, one would expect water (and also other non-refractory species as CH_4 , NH_3 , CO ..., grouped within the denomination of “ices”) to be in vapor or fluid form in the planet. One possibility that we must consider however is that the planet may have formed at large orbital distances and be brought in close to its parent star relatively late.

From the phase diagram of H_2O (Fig. 1) it is clear that with an effective temperature above 1000 K, the planet

would be composed of supercritical water. If the planet follows an adiabat, it will remain in vapor form transforming eventually into a plasma. If instead, the planet had an effective temperature below the melting point of water (e.g. because it formed far from the central star), it will exhibit different high pressures forms of ice, up to a regime where ice VII and ice X (for the massive icy planets) dominate.

The EOS used for steam (water vapor) is obtained from a combination of data obtained from a finite temperature molecular dynamics (FT-DFT-MD) simulation by French et al. (2009) and of the Sesame 7150 EOS (see Kerley 1972). The FT-DFT-MD data are used for $T = 1000 - 10,000$ K and $\rho = 2 - 7$ g cm $^{-3}$ as well as for $T = 10,000 - 40,000$ K and $\rho = 5 - 15$ g cm $^{-3}$. Sesame 7150 data are used elsewhere. The two EOS are joined by interpolation of isotherms.

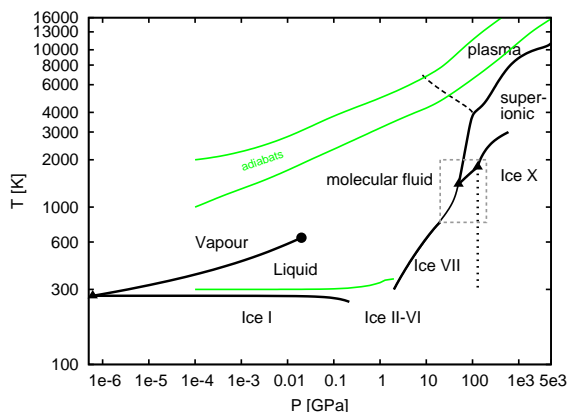


Fig. 1. Phase diagram of water from 0.01 bar to 50 Mbar and 300 to 16000 K. *Black solid lines*: phase-transition boundaries, *Triangles*: Triple points, *Circle*: critical point; *grey solid lines*: adiabats starting from 300, 1000, and respectively 2000 K at 1 bar; *black dashed line*: continuous transition from molecular dissociated water to water plasma; *grey dashed box*: region of high uncertainty and contradictive experimental and theoretical results. For $P > 4$ GPa and $T \geq 1000$ this diagram relies on data from FT-DFT-MD calculations French et al. (2009). The melting curve is taken from Feistel et al. (2006), the saturation curve from Wagner & Pruß (2002), and the phase boundary of Ice VII is adapted from Goncharov et al. (2009) for pressures lower than 30 GPa. For higher pressures, experimental and theoretical investigations predict different phase boundaries Ice VII–molecular water, Ice VII–superionic water, Ice VII–Ice-X (controversial as a hard boundary from experiments (Hemley et al., 1987)), IceX–superionic water and different locations of corresponding triple points French et al. (2009); Goncharov et al. (2009); Schwager et al. (2004).

3.2.3. Silicates

The dominant constituents in the mantles of the terrestrial planets are silicates with a high (i.e. 0.90) magnesium number ($X_{\text{Mg}} = \text{Mg}/(\text{Mg}+\text{Fe})$). This is a consequence of early formation, when the part of Fe that remained immiscible

differentiated to form the core. Even though the composition of extra-solar Earths may largely vary in this number, our starting point is to consider a composition similar to that of Earth, and thus we show the relevant phases in Fig. 2. The diagram shows primarily the forsterite (Fo: Mg_2SiO_4), perovskite/post-perovskite (pv/ppv: MgSiO_3), magnesiowustite (mw: MgO) system.

We show two adiabats calculated at 300 K and 2000 K and 1 bar for comparison. Both melting curves of pv and mw show a steep slope that can pose a barrier to melting of the interior. Given that we do not know the melting behaviour of post-perovskite or of MgO at large pressures, it remains unclear if the lower-most mantle of super-Earths can easily melt or not.

It should be noted that melting will depend on the amount of iron in the mantle (i.e. the magnesium number), but also on the abundance of minor species, something not included in Fig. 2. As an example, on Earth, decompression melting can occur at temperatures around 1300K (Hirschmann, 2000). We do not attempt to determine the fraction of the planet’s surface that may be molten, but note that it may be relatively large.

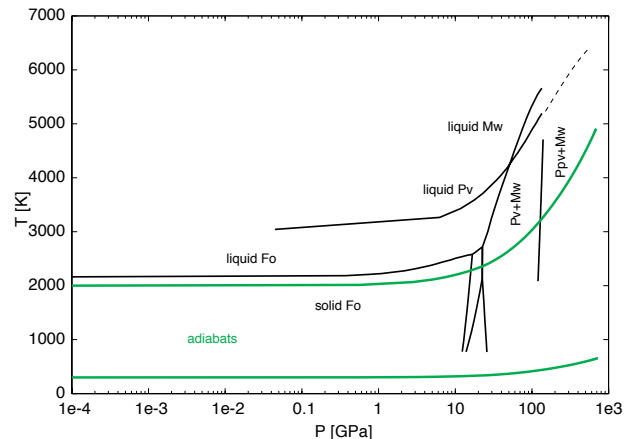


Fig. 2. Simplified $P - T$ phase diagram for relevant silicates on super-Earths. Data is taken from Presnall (1995) for the Mg-silicate end member, with phase boundaries for solid forsterite (dominant in the upper mantle), to Earth’s lower mantle materials, perovskite (pv) and magnesiowustite (mw). The melting curve for pv and mw, which remains controversial, are shown, as well as an extrapolation of the pv’s melting curve to higher pressures. The phase boundary of post-perovskite (ppv) was calculated from Tsuchiya et al. (2004). Adiabats at 300 K and 2000 K and 1 bar are shown for reference.

3.2.4. Iron

We also considered the unlikely scenario of a planet made of pure iron. This provides the upper limit on the mass of a transiting planet. The adiabats shown were calculated from the thermodynamic data derived by Uchida et al. (2001) in a pressure range of 8-18 GPa and a temperature range of 298-973 K. The shallow nature of the adiabats is a consequence of the extrapolation of this data. However, the

melting boundary (derived from results from ab-initio calculations by Morard et al. (2009)) is quite steep so that pure-iron planets are likely to be mostly solid. However, the state of the core may be molten in planets that have a mantle due to its insulating character that would keep the core at higher temperatures.

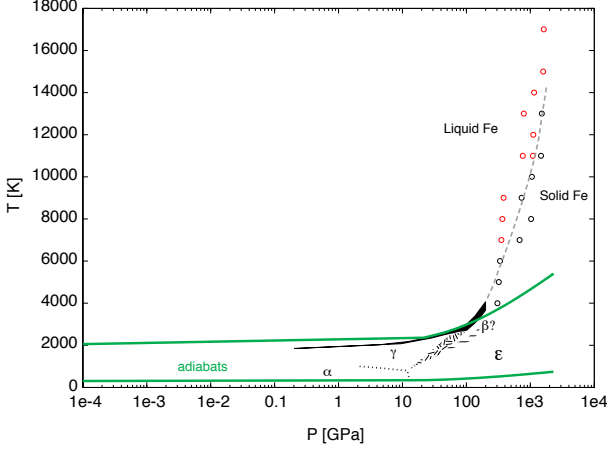


Fig. 3. $P - T$ phase diagram for iron. Values for pressures below 200 GPa were adapted from Boehler (2000) and references therein. The black region shows the agreement in the melting curve of iron at relatively low pressures. Data points for melting in the high pressure regime of 306-1625 GPa are from Morard et al. (2009). Red points correspond to the liquid phase, while black points are solid Fe. The dash curve is a melting line drawn to approximate the boundary suggested by the results from the ab-initio calculations. Adiabats from 300K and 2000K and 1bar were extrapolated with the thermodynamic data (gruneisen parameters and debye temperature) derived by Uchida et al. (2001) in a low pressure regime (8-18 GPa).

4. Inferring Composition

4.1. CoRoT-7b as a terrestrial (iron+rock) planet

4.1.1. Description

We first consider CoRoT-7b to be a planet similar in interior composition to Mercury, Earth, Venus or Mars, i.e. that it is made of a silicate mantle on top of an iron core. Given the planet's proximity to its star and the large evaporation rate (derived in §2), this is by far the most likely possibility.

4.1.2. The atmosphere

Because of its proximity to the central star, the planet's surface may be heated to extremely high temperatures. Given the star's characteristics ($T_{\text{eff}} = 5275 \text{ K}$, $R_{\star} = 0.87 R_{\odot}$) and planet's semi-major axis ($a = 4.27 R_{\star}$), the effective equilibrium temperature at the planet's substellar point is (assuming a zero albedo) $T_{\text{eq}}^{\text{sub}} = 2570 \text{ K}$. Distributed evenly on the planet's surface, this temperature is $T_{\text{eq}}^{\text{global}} = 1820 \text{ K}$.

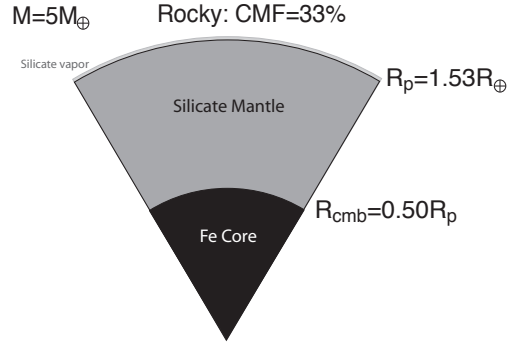


Fig. 4. Drawing to show the interior structure envisioned for a planet made of iron and rocks. The composition is Earth-like with a core-mass fraction (CMF) of 33%.

Even though the exact temperature depends on the emissivity and albedo, it is clear that silicates (or iron if present at the surface) should be molten by the intense heat, at least on part of the planet for temperatures above 2000 K (see Figs. 2 and 3).

A first consequence of a molten surface is that volatiles should be efficiently outgassed from the planetary interior (e.g. Schaefer & Fegley, 2007). However, because the total mass of those volatiles would be as small as at most a few 10 % of the planet's mass, this is a temporary effect and given the significant mass loss, the massive atmosphere thus formed should disappear quickly (on a timescale of $10^6 - 10^8$ yrs, based on the arguments in §2). The remaining planet should then contain only refractory material, with vapor in equilibrium with the lava, and an evolving composition as a function of the mass loss.

Specific models for the chemistry of the atmosphere of evaporating silicate super-Earths (Schaefer & Fegley, 2009) indicate that a planet such as CoRoT-7b with a composition similar to that of the bulk silicate Earth would have an equilibrium atmosphere with a pressure initially between 10^{-6} and 10^{-2} bars (corresponding to our range of extreme temperatures). The evaporating vapor atmosphere should be mainly composed of Na, then SiO, O and O₂, then Mg, as the less refractory species are progressively lost. Schaefer & Fegley (2009) find that the pressures decrease by about 1 order of magnitude when Na is lost, and then by a further 2 to 3 orders of magnitude at 90% of total erosion.

With such a thin atmosphere, the planetary radius measured from the transits can be considered as that of the solid/liquid surface of the planet.

4.1.3. Limits to the mass loss?

Compared to the arguments presented in §2, the planet's erosion may be reduced if (i) UV photons are not fully absorbed in the atmosphere but hit the surface of the planet, or (ii) the "supply" of atmosphere is slowed by the need to deliver heat to pass the latent heat barrier.

The photoionization cross-section of atomic species such as H, O, Fe, Mg, Si is between $\sigma_{\text{UV}} \approx 10^{-19}$ and 10^{-17} cm^2 in the 10-50 eV energy range (Verner et al., 1996). The unit optical depth for UV photons corresponds to a pressure $P_{\text{UV}} = \mu m_p g / \sigma_{\text{UV}}$, where μ is the mean molecular weight of the atmosphere, m_p the proton's mass and g the planet's gravity. Using $g \approx 1000 \text{ cm s}^{-2}$ and $\mu \approx 10 \text{ g}$ one finds

$P_{UV} \approx 10^{-7}$ to 10^{-9} bar. (For comparison, $P_{UV} \approx 10^{-9}$ bar for gas giants -see Murray-Clay et al. (2009)).

Because those values of P_{UV} are much smaller than those of the vapor pressure estimated above, it appears that the equilibrium vapor atmosphere is able to efficiently absorb stellar UV photons that will drive the escape from the planet. Note however that the precise rate of escape depends on cooling processes and hydrodynamical modeling much beyond the scope of this work.

Let us now consider whether a bottleneck to the escape may be caused by the need to vaporize material that is initially solid or liquid. In order to do so, we balance the energy required for the sublimation at a rate \dot{M}_{sub} with the absorbed heat flux $\pi R_p^2 F_\star$, where F_\star is the stellar irradiation. Note that F_\star is formally the stellar flux that reaches the ground, but given the thinness of the atmosphere, this is equivalent as the irradiation flux at the top of the atmosphere. The sublimation rate can hence be written:

$$\dot{M}_{\text{sub}} = \frac{\pi R_p^2 F_\star}{\mathcal{L}_{\text{sub}}}, \quad (8)$$

where \mathcal{L}_{sub} is the latent heat of sublimation. Using $\mathcal{L}_{\text{sub}} \approx 10^9 - 10^{10}$ erg g $^{-1}$ K $^{-1}$ (typical for iron and silicates), we find $\dot{M}_{\text{sub}} \approx 10^{17}$ to 10^{18} g s $^{-1}$, i.e. at least 6 orders of magnitude larger than the mass loss we previously derived. Hence, there is no mass loss suppression due to latent heat effects.

We thus conclude that at this orbital distance (less than 5 stellar radii away from its star) the planet may erode even if made of the most refractory materials!

4.1.4. Possible compositions and masses

We explore the case in which the planet is of telluric composition. The largest size for a rocky planet is when it is made only of silicates (i.e. coreless planet). On the other hand, the smallest size corresponds to a pure Fe-planet. However, a planet is unlikely to form as a pure iron ball. During the condensation of the solar nebula, iron and silicates are condensed out at similar temperatures so that if iron is present, so are silicates, especially in large objects. Given an abundance of oxygen, there would not be a limit to forming mantle minerals. Thus the largest core a planet can form is one congruent with a Fe/Si nebula ratio (of ~ 0.63 for a sunlike star). However, secondary processes like giant impacts and erosion can produce planets with large core mass fractions.

Considering the measured radius of CoRoT-7b, including the uncertainty, the smallest mass is $\sim 4 M_\oplus$ for a pure silicate composition (see Fig. 5). If its mass is measured to be less than this value, it would mean that the planet contains a considerable amount of volatiles.

On the other hand, the absolute upper limit in mass is $\sim 25 M_\oplus$ corresponding to a pure Fe-planet. We now turn to investigate whether or not planets can completely lose their silicate mantles through evaporation and end up as pure iron planets.

We consider planets with initial masses of 15, 10 and 5 M_\oplus and an Earth-like composition (33% iron core, 67% mantle rock). We integrate Eq. 1, with the adequate density found from calculating the planet's structure at each time step. The chosen efficiency for this calculation is $\epsilon = 0.1$. The results are shown in Fig. 6. We find that small planets

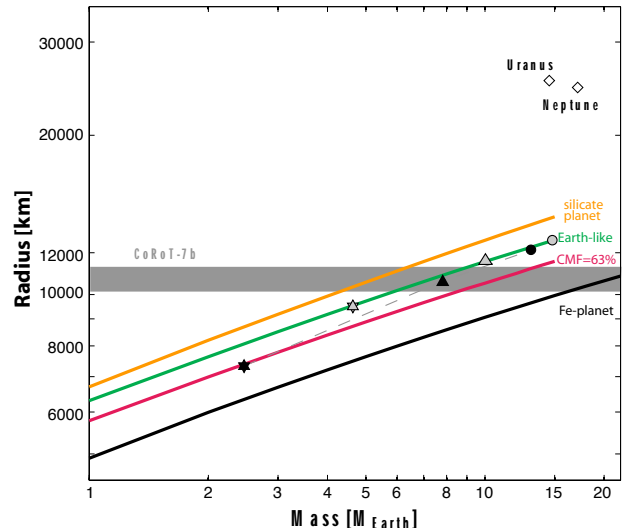


Fig. 5. Mass-radius relations for planets made of iron and rocks. The compositions considered are pure iron, 63% core and 37% mantle, 33% core and 63% mantle corresponding to an Earth-like planet, and 100% silicate mantle planet. Initial radii for a 5- M_\oplus planet (grey star), 10- M_\oplus (grey triangle) and 15- M_\oplus (grey circle) planets with Earth-like composition. Corresponding filled symbols show the mass and radius after 3 Ga of silicate mass loss according to Eq. 1.

suffer a larger atmospheric loss, due to the inverse dependence on average density. Also, as planets lose their silicate mantles, their average density either increases (for small planets) or stays relatively constant (for massive planets) owing to a cancelling effect between a reduction in size and mass. Thus, the rate of atmospheric loss decreases through time. Interestingly, all three planets after 3 Ga lose a similar amount of mass, between 2 and 2.5 M_\oplus , which is significant for a planet that starts small. For example, a 5 M_\oplus -planet that starts with the core being 1/3 of its total mass, after 3 Ga loses 3/4 of its mantle. Consequently it increases its core fraction to 2/3. Conversely, initially massive rocky super-Earths will lose less proportion of mantle mass and will not increase their core fraction significantly. Therefore, it is especially difficult to find massive ($> 10 M_\oplus$) pure-iron planets. Being that the formation limit of 63% core can not be significantly increased for massive planets, the upper limit in mass for CoRoT-7b is $\sim 15 M_\oplus$.

4.2. CoRoT-7b as an iron-rock-ice planet

4.2.1. Description

Although now very close to its star, the planet may have formed at large distances and migrated inward, either early in the first million years when a circumstellar gaseous disk was still present (e.g. Lin et al., 1996), or later, for example because of another companion and a Kozai mechanism with tides that may have led to a progressive inward migration (e.g. Wu & Murray, 2003).

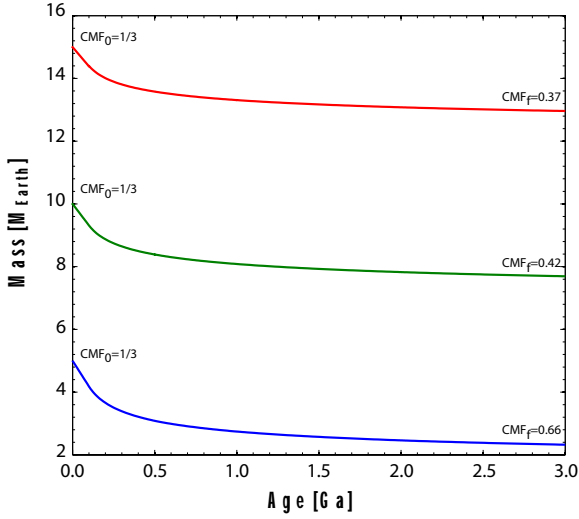


Fig. 6. Evolution in mass of an Earth-like planet with initial mass of 5, 10 and 15 M_{\oplus} . The mass loss is calculated from Eq. 3. The initial and final proportions of core mass fraction are shown.

Let us consider a planet of $M_p = 10 M_{\oplus}$ made mostly of water (for simplicity). The gravitational energy transformed into internal energy during its formation is $E_i \approx 3/10 GM_p^2/R_p$. In the absence of irradiation (if far enough from the star), the planet is initially made of steam. If steam is present in the photosphere (i.e. without an optically thick layer of hydrogen and helium), it will maintain a high atmospheric temperature (and therefore a rapid cooling) until complete condensation of water onto the interior is reached. Given an effective temperature (as obtained from the temperature at which the saturated vapor pressure (e.g. Emmanuel, 1994) is equal to the photospheric pressure, $P_{\text{vap}}(T) = 2/3 g/\kappa$), an upper limit to the time to solidification is $\tau_{\text{solid}} = E_i/(4\pi R_p^2 \sigma T_{\text{eff}}^4)$, i.e. for $R_p \approx 15,000$ km, $\tau_{\text{solid}} \approx 100$ Ma when using a low opacity $\kappa = 10^{-2} \text{ cm}^2 \text{ g}^{-1}$ ($T_{\text{eff}} \approx 320$ K). On the other hand, if ice grains and/or water droplet in the atmosphere prevent it from cooling efficiently, $\kappa \approx 10^2 \text{ cm}^2 \text{ g}^{-1}$ ($T_{\text{eff}} \approx 210$ K) so that $\tau_{\text{solid}} \approx 1$ Ga.

At least in theory, there is thus a (small) possibility that CoRoT-7b is a planet that was formed at large distances from the star, had sufficient time (hundreds of millions of years) to solidify before being brought to an orbital distance of 0.017 AU, where ice would be sublimating again.

4.2.2. The atmosphere

As the planet moves inward, its icy surface will sublimate to form a vapor atmosphere. The thickness of this atmosphere will be controlled by the ability of stellar photons to reach the planetary surface and the balance between the sublimation rate of the icy surface and the loss rate of the vapor atmosphere (see also Kuchner, 2003).

The balance between the irradiation luminosity and rate of energy required for sublimation has been described in

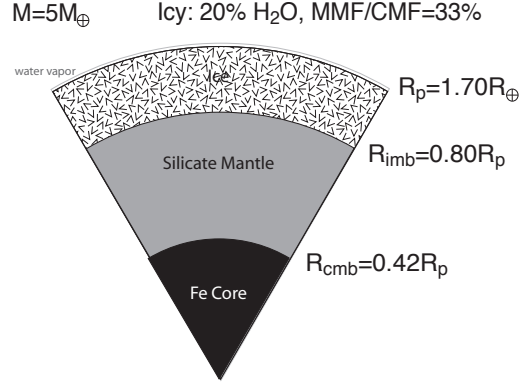


Fig. 7. Drawing to show the interior structure envisioned for a planet made of iron, rocks and solid ice. This composition has the same ratio of Si/Fe as for Earth, plus an additional 20% by weight of H_2O in ice form.

the case of the silicate planet (eq. [8]). However, the specific energy H required for the sublimation now needs to include a heating term: $H \equiv \mathcal{L}_{\text{sub}} + c_p(T_{\text{sub}} - T_{\text{ini}})$, where c_p is the specific heat at constant pressure. Since $T_{\text{sub}} - T_{\text{ini}}$ is at most ~ 100 K, we use $H = 3 \times 10^{10} \text{ erg g}^{-1}$, slightly above the value for the latent heat of ice (Podolak et al., 1988).

A second complication is that we have to estimate the amount of flux that indeed reaches the surface:

$$F_v = \frac{L_*}{4\pi a^2} e^{-\tau}, \quad (9)$$

where a is the semi-major axis, L_* is the stellar luminosity ($= 0.53 L_{\odot}$ for CoRoT-7) and τ is the atmosphere's optical depth at visible wavelengths. The sublimation mass can hence be written:

$$\dot{M}_{\text{sub}} = \frac{L_*}{H} \left(\frac{R_s}{2a} \right)^2 e^{-\tau}. \quad (10)$$

The optical depth τ is obtained by equating \dot{M}_{sub} and \dot{M}_{esc} (i.e., eqs. [1] and [10]) and $\tau \simeq 14$ with values characteristic of CoRoT-7b.

The atmospheric pressure is

$$P_s \simeq \frac{g}{\kappa} \tau = 0.02 \left(\frac{M_p}{3M_{\oplus}} \right) \left(\frac{R_s}{1.7R_{\oplus}} \right)^{-2} \text{ bar}, \quad (11)$$

with $\tau = 14$ and $\kappa = 0.6 \text{ cm}^2 \text{ g}^{-1}$, the water opacity at 10000 cm^{-1} (Guillot et al., 1994; Freedman et al., 2008). The vapor mass, M_{vap} , is related to the atmospheric pressure in such a way that $P_s = M_{\text{vap}} g / 4\pi R_s^2$. Thus,

$$\frac{M_{\text{vap}}}{M_p} = 2 \times 10^{-8} \left(\frac{M_p}{3M_{\oplus}} \right)^{-1} \left(\frac{R_s}{1.7R_{\oplus}} \right)^2 \quad (12)$$

The physical thickness of the atmosphere can be estimated as follows. For simplicity we consider a polytropic atmosphere without self-gravity. Then, integration of the equation of hydrostatic equilibrium from the surface to the visible photosphere yields

$$\frac{R_{\text{ph}} - R_s}{R_s} = \frac{1}{\lambda_{\text{ph}} \nabla} \left[\left(\frac{P_s}{P_{\text{ph}}} \right)^{\nabla} - 1 \right], \quad (13)$$

where R_{ph} and P_{ph} are the photospheric radius and pressure, ∇ is the adiabat, and

$$\lambda_{\text{ph}} = \frac{GM_p \rho_{\text{ph}}}{R_{\text{ph}} P_{\text{ph}}}; \quad (14)$$

is the ratio of the photospheric radius to the pressure scale height. With the equation of state of ideal gas, λ_{ph} comes out to

$$\lambda_{\text{ph}} = 120 \left(\frac{M_p}{3M_{\oplus}} \right) \left(\frac{R_{\text{ph}}}{1.7R_{\oplus}} \right)^{-1} \left(\frac{T_{\text{ph}}}{2000\text{K}} \right)^{-1} \left(\frac{\mu}{18} \right). \quad (15)$$

Since $P_s/P_{\text{ph}} \simeq \tau (\simeq 14)$ and $\nabla \simeq 0.15$, the height of the photosphere, $R_{\text{ph}} - R_s$, $\sim 0.03R_s$. The transit radius is slightly larger than the photospheric radius; its excess radius, ΔR , is given by (Burrows et al., 2007)

$$\frac{\Delta R}{R_{\text{ph}}} = \lambda_{\text{ph}}^{-1} \ln \sqrt{2\pi\lambda_{\text{ph}}}. \quad (16)$$

Using Eq. (15), one obtains $\Delta R \sim 0.03R_{\text{ph}}$. Given other uncertainties, this effect is small and will not be included in the analysis below.

4.2.3. Possible compositions and masses

We compute the structure of different mixtures of ices, mantles and iron cores, for different masses and obtain a 'to-blerone' diagram (triangular prism) that relates mass, composition and size (Valencia et al., 2007b). We then project onto a ternary diagram the compositions that would conform to a measured radius ($R=1.68$) for different masses. The result is shown in Fig. 8, where the degeneracy in composition is evident. It shows the range in compositions for each value of mass (iso-mass lines). If CoRoT-7b was cold, its mass could not be less than $2M_{\oplus}$, and if less than $4M_{\oplus}$ (once the uncertainty in the radius is included), it would mean the planet necessarily was an icy one.

4.3. CoRoT-7b as a steam planet

4.3.1. Description and possible origin

If CoRoT-7b formed at large orbital distances and accreted both ices and hydrogen and helium (similarly to Uranus and Neptune) or if it accreted only ices but migrated rapidly in the disk phase, it is likely that it was unable to get rid of its internal heat and solidify. Its structure may therefore be similar to those of Uranus and Neptune: a fluid interior with a mass-radius relation that departs significantly from that of a solid planet.

We now seek to provide limits to the presence of steam (water vapor) and hydrogen and helium in CoRoT-7b.

4.3.2. Constraints on the presence of steam

To estimate possible amounts of steam compatible with the measurements of CoRoT-7b, we proceed as follows: First, for simplicity, we only consider the case of a solid/liquid interior that is "Earth-like" in composition (33% iron core, 67% mantle rock) and surrounded by an envelope of pure water vapor (steam). Our calculations of interior models

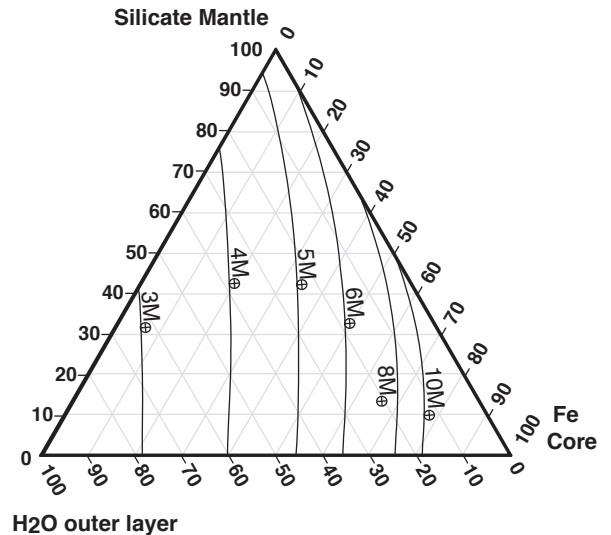


Fig. 8. Ternary diagram for a cold planet with $R=1.68 R_{\oplus}$

Each point in the diagram depicts a unique mixture of iron cores, silicate mantles and ices. Each vertex represents 100% of each compositional end-member and the opposite side represents a 0% value. The lines for constant mass values are shown. Masses of less than $2M_{\oplus}$ are unrealistic for a solid CoRoT-7b.

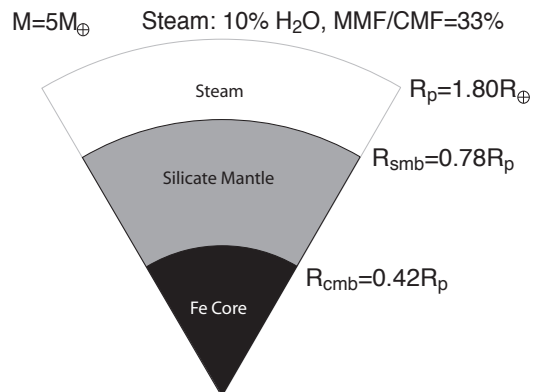


Fig. 9. Drawing to show the interior structure envisioned for a planet made of iron, rocks and steam (possibly with H-He)

for the iron+rock part as a function of its mass $M_{\text{Fe+R}}$ and outside pressure P_0 were found to yield radii of order:

$$R_{\text{Fe+R}} = 6910 \text{ km} \left(\frac{M_{\text{Fe+R}}}{5M_{\oplus}} \right)^{0.27 + \log_{10} P_0 / 100} 10^{-(\log_{10} P_0 / 7)^3}, \quad (17)$$

where P_0 is in GPa units. The relation is only an approximation found to be accurate to 2% for $M_{\text{Fe+R}}$ between 1 and $10M_{\oplus}$ and P_0 between 1 and 10^4 GPa ($= 100$ Mbar).

The size of the planet with steam is found by calculating the evolution of an initially adiabatic planet with a specific entropy equal to that of steam at 10 bar and 2500 K.

This initial state is chosen as representative of any "hot start", since any evolution from still higher entropies would

have been fast. We neglect any possible orbital evolution of the planet.

The evolution is characterized by the rapid growth of a radiative zone just below the atmospheric boundary, similarly to what is obtained for giant exoplanets (Guillot, 2005). This zone quickly becomes isothermal and extends down to pressures around 10 kbar, and temperatures ~ 3000 K. At those pressures and temperatures, the rapid rise in radiative opacities implies that any further extension of the radiative region must wait for a large reduction of the intrinsic luminosity, implying a slow cooling. This implies that results should be relatively robust, in regard of uncertainties in initial state, opacities, age...etc.

Figure 10 shows the resulting planetary radii after 2 Ga of evolution for various mass fractions of steam in the planet. The presence of an atmosphere of steam is found to affect the structure and size of the planet relatively significantly. For a composition of more than 50% steam, we find that radii are always above the 1σ upper limit obtained for CoRoT-7b, whatever the planetary mass that is considered. When considering masses above $4M_{\oplus}$ we find that the upper limit on the amount of steam present is $\sim 20\%$, i.e. around $1M_{\oplus}$. This implies that the quantity of steam is limited. Given the relatively significant evaporation rate (§ 2), it is relatively unlikely that we may be observing it now, but this possibility cannot be ruled out.

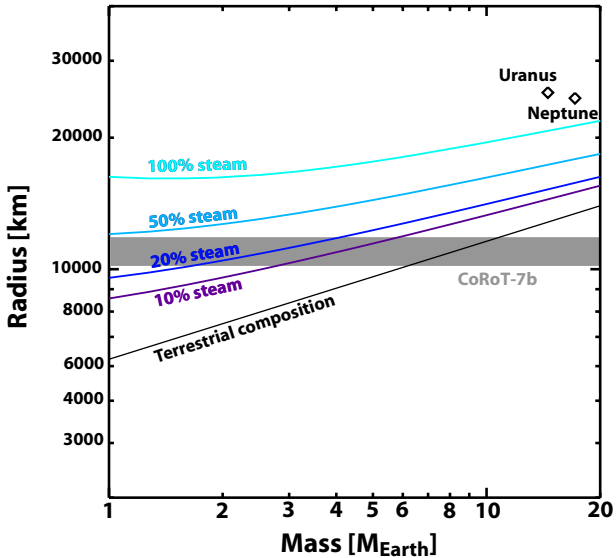


Fig. 10. Radius as a function of mass for a planet made of iron, rocks and steam. The “terrestrial composition” line corresponds to the limiting value of a planet without steam. Other lines corresponds to total mass fraction of steam from 10% to 100% (planet made of pure water). Except for the latter case, the fraction of iron to rocks is 33%. The models with steam have been evolved for 1 Ga using our fiducial opacity table (see text). Radii correspond to the 10 bar level.

4.3.3. Constraints on the presence of hydrogen and helium

With the same method, we derive constraints on the amounts of hydrogen and helium that may be present. Figure 11 shows that any hydrogen and helium leads to a very significant increase in the size of the planet. For the two calculations that we perform (10% and 2% of hydrogen and helium), the radii that we obtain are always much larger than that of CoRoT-7b. Because of the low gravity and high compressibility of the envelope, we find that planets with smaller masses have larger radii if they contain a H-He envelope and are significantly irradiated. We infer that CoRoT-7b may possess an envelope of hydrogen and helium that is much less than 1% of the total planetary mass. As in the case of steam (but even more so), we conclude that it is extremely unlikely that CoRoT-7b possesses an atmosphere of hydrogen and helium.

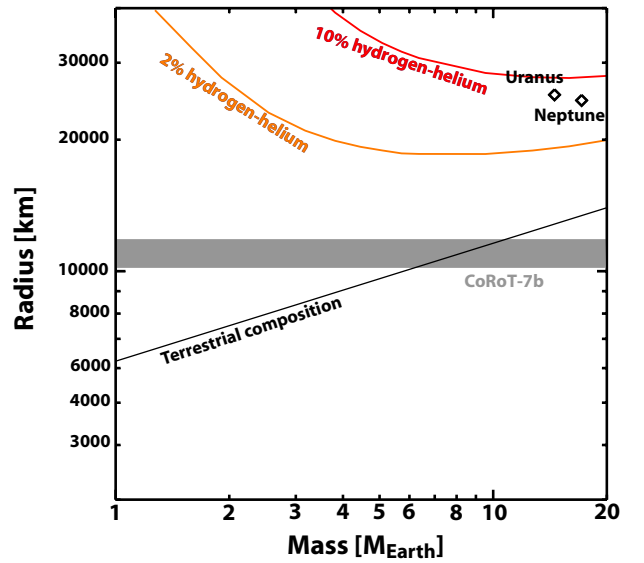


Fig. 11. Radius as a function of mass for a planet made of iron, rocks and hydrogen and helium in solar proportions. The “terrestrial composition” line corresponds to the limiting value of a planet without steam. Other lines corresponds to total mass fraction of hydrogen and helium of 2% and 10%, respectively, to 100% (planet made of pure water). Except for the latter case, the fraction of iron to rocks is 33%. The models with steam have been evolved for 1 Ga using our fiducial opacity table (see text). Radii correspond to the 10 bar level.

4.3.4. CoRoT-7b as an evaporated ice or gas giant?

We now examine whether CoRoT-7b may have been formed by outstripping a gas giant or an ice giant from its envelope, leaving a planet with little or no gaseous envelope. In order to do so, we first calculate an ensemble of evolution models with a constant total mass and a constant composition. This ensemble of models is characterized by a unique “core” (iron+rock) mass, and variable total masses (from 10 to about $120M_{\oplus}$). The combined mass and ther-

mal evolution of a planet with mass loss is then calculated by noting that for each planetary mass and central specific entropy corresponds a given planetary radius, and therefore a given mass loss, and that central entropy should be conserved during mass loss:

$$\frac{dM}{dt} = f(\rho_p), \quad (18)$$

$$\frac{dS_c}{dt} = \left(\frac{\partial S_c}{\partial t} \right)_M, \quad (19)$$

where $f(\rho_p)$ is a function of the planet's density provided by eq. 3, and the loss of central entropy S_c is calculated from individual evolution models with fixed mass.

The results are shown in Fig. 12. For planets that are initially ice giants with no hydrogen and helium that migrated to the present orbital distance rapidly (within ~ 100 Ma), using our fiducial mass loss efficiency parameter ($\epsilon = 0.1$), we find that a maximum possible initial mass is around $17 M_\oplus$, i.e. the mass of Neptune. Indeed, for planets that are initially hot and extended, mass loss proceeds rapidly. For planets that are made of hydrogen and helium, their large radius yields a very rapid loss of their envelope: mass loss is inversely proportional to the planet's density. We therefore find that a planet with a small core ($\sim 10 M_\oplus$ or less) may have eroded to become CoRoT-7b whatever its initial composition in hydrogen and helium.

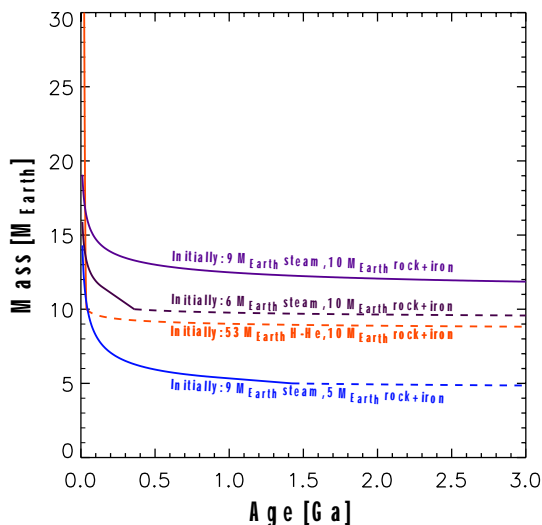


Fig. 12. Evolution in mass of a steam planet with initial conditions as labelled. The mass loss is calculated from Eq. 3. The dashed lines correspond to periods for which the entire steam/gaseous atmosphere has been lost and the solid/liquid planet is being eroded.

From the point of view of interior and evolution models, there is thus a range of possibilities to explain the characteristics of CoRoT-7b: it may have been initially a gas giant planet that was eroded down to its dense core, it may have been a Uranus-like ice giant which would have lost most or

all of its “ices”, or it may have been all the way a rocky planet with no ice or hydrogen and helium.

5. Conclusion

CoRoT-7b is the first of possibly many extreme close-in super-Earths that will be discovered in the near future. We have shown that the atmospheric escape for this type of planets is expected to be high, within an order of magnitude of that of HD 209458 b, and mostly independent of composition. A simple analysis shows that for CoRoT-7b, the mass already lost to escape would be of order $\sim 3 M_\oplus$, possibly much more if the planet initially contained a massive hydrogen-helium envelope.

By considering three scenarios for composition we arrive at upper limits on the volatile content. The first case is that the planet formed far, accumulated substantial amounts of ice, was able to cool and solidify, then migrated in evaporating part of its icy layer. The lower limit in mass for an icy CoRoT-7b is $2 M_\oplus$.

Another possibility is that the planet was initially an ice giant that during migration lost most of its volatile content. The maximum amount of water vapor (steam) for CoRoT-7b would then be 20% by mass. The planet may have been initially been as massive as Neptune and lost most, if not all of its water and volatile species. Similarly, the precursor of CoRoT-7b may have been a gas giant, in which case the present amount of hydrogen and helium is constrained to be less than 1%. This low limit combined to the significant mass loss rate imply that it is extremely unlikely that CoRoT-7b contains a significant proportion of hydrogen and helium.

Evidently, a natural and likely possibility is that CoRoT-7b is a terrestrial planet with a thin silicate vapor atmosphere. For a planet similar to the Earth in composition, we would expect for CoRoT-7b's size a mass between 6 and $9.5 M_\oplus$. Accounting for mass loss and an initial Earth-like composition, the present core mass fraction may be of order 40% for big planets and 67% or more for the smaller ones. This implies a likely mass between 7 and $15 M_\oplus$. It is important to note that as a result of lower erosion rates for dense planets, it is very unlikely to find a massive pure-iron super-Earth. For any possible composition, the ensemble of solutions for iron+rock planets is compatible with masses between 4 and $15 M_\oplus$.

A key information will be the measurement of the mass of the planet by radial velocity. Clearly, our models indicate a vast range of possibilities, from 2 to $15 M_\oplus$, but the knowledge of the planetary mass will allow ruling out possible compositions. Most importantly the discovery of similar planets in different configurations will be crucial to understand the origin and fate of what may be a new class of planets.

In parallel, the mass loss that we infer implies that there is a possibility to probe for the composition of the outer shell of the planet by measuring the composition of the extended planetary exosphere. CoRoT-7 ($V = 11.7$) is significantly fainter than HD209458 ($V = 7.65$), so that the measurement is challenging. However, the fact that a detection of escaping H, C and O is possible for HD 209458 b (Vidal-Madjar et al., 2003, 2004) yield great hopes for similar measurements for CoRoT-7b and close-in super-Earths in the nearby future.

Acknowledgements. We would like to thank Guillaume Morard and colleagues for making their data available before publication. This research was carried out as part of a Henri Poincaré Fellow at the Observatoire de la Côte d’Azur to DV. The Henri Poincaré Fellowship is funded by the CNRS-INSU, the Conseil General des Alpes-Maritimes and the Rotary International -District 1730. MI got financial support from Program for Promoting Internationalization of University Education from the Ministry of Education, Culture, Sports, Science and Technology, Japan, and from the *Plan Pluri-Formation* OPERA. The authors acknowledge CNES and the CNRS program *Origine des Planètes et de la Vie* for support. The authors further thank the CoRoT community, Didier Saumon, Bruce Fegley for discussions and sharing results in advance of publication.

References

- Adams, E., Seager, S., & Elkins-Tanton, L. 2008, *ApJ*, 673, 1160
- Alexander, D. R., & Ferguson, J. W. 1994, *ApJ*, 437, 879
- Boehler, R. 2000, *Rev. Geophys.*, 38, 221
- Burrows, A., Hubeny, I., Budaj, J., & Hubbard, W. B. 2007, *ApJ*, 661, 502
- Emmanuel, K. 1994, in “Atmospheric Convection”, Oxford Univ. Press, Oxford
- Erkaev, N. V., Kulikov, Y. N., Lammer, H., Selsis, F., Langmayr, D., Jaritz, G. F., & Biernat, H. K. 2007, *A&A*, 472, 329
- Feistel, R., Wagner, W., J. 2006, *Phys. Chem. Ref. Data*, 35, 1021
- Freedman, R. S., Marley, M. S., & Lodders, K. 2008, *ApJS*, 174, 504
- French, M., Mattsson, T.R., Nettelmann, N., & Redmer, R. 2009, *Phys. Ref. B* 79, 054107
- García Muñoz, A. 2007, *Planet. Space Sci.*, 55, 1426
- Goncharov, A.F. et al. 2009, *J. Chem. Phys.*, 130, 124514
- Guillot, T. 2005, *Annual Review of Earth and Planetary Sciences*, 33, 493
- Guillot, T., Gautier, D., Chabrier, G., & Mosser, B. 1994, *Icarus*, 112, 337
- Guillot, T., & Morel, P. 1995, *A&AS*, 109, 109
- Guinan, E. F., & Engle, S. G. 2009, arXiv:0901.1860
- Guinan, E. F., & Engle, S. G. 2007, arXiv:0711.1530
- Hemley, R. J., Jephcoat, A. P., Mao, H. K., Zha, C. S., Finger, L. W., & Cox, D. E. 1987, *Nature*, 330, 737
- Hirschmann, M. M., 2000. Mantle solidus: Experimental constraints in the effects of peridotite composition. G-cubed 1.
- Hodgkin, S. T., & Pye, J. P. 1994, *MNRAS*, 267, 840
- Ikoma, M. & Genda, H. 2006, *ApJ*648, 696
- Iro N., Bézard B., & Guillot T. 2005, *A&A*, 436, 719
- Kuchner, M. J. 2003, *ApJ*, 596, L105
- Lakatos, S. L., Voyer, E. N., Guinan, E. F., DeWarf, L. E., Ribas, I., & Harper, G. M. 2005, *Bulletin of the American Astronomical Society*, 37, 442
- Lecavelier des Etangs, A., Vidal-Madjar, A., McConnell, J. C., & Hébrard, G. 2004, *A&A*, 418, L1
- Leger, A., Rouan, D., Schneider, R. et al. 2009, *A&A*, submitted
- Lin, J., Gregoryanz, E. Struzhkin, V. 2005, *GRL*, 32, 11306
- Lecavelier Des Etangs, A. 2007, *A&A*, 461, 1185
- Lin, D. N. C., Bodenheimer, P., & Richardson, D. C. 1996, *Nature*, 380, 606
- Morard, G., Guyot F., Bouchet J., & Mazevet S. 2009, *EPSL*, submitted
- Murray-Clay, R. A., Chiang, E. I., & Murray, N. 2009, *ApJ*, 693, 23
- Penz, T., et al. 2008, *Planet. Space Sci.*, 56, 1260
- Podolak, M., Pollack, J. B., & Reynolds, R. T. 1988, *Icarus*, 73, 163
- Presnall, D. C., 1994, *Phase Diagram of Earth-Forming Minerals*, in *Mineral Physics and Crystallography A Handbook of Physical Constants*, ed. Ahrens, T. J. (AGU), 354
- Ribas, I., Guinan, E. F., Güdel, M., & Audard, M. 2005, *ApJ*, 622, 680
- Saumon, D., Chabrier, G., & van Horn, H. M. 1995, *ApJS*, 99, 713
- Schaefer, L., & Fegley, B. 2007, *Icarus*, 186, 462
- Schaefer, L., & Fegley, B. 2009, submitted to *ApJL* [astro-ph:0906.1204]
- Schwager, B., Chudinovskikh, L., Gavriiliuk, A., & Boehler, R. 2004, *J. Phys.: Condensed Matter*, 16, 1177
- Schwegler, E., Sharma, M., Gygi, F., & Gallir, G. 2008, *PNAS*, 105, 14779
- Tian, F., Kasting, J. F., Liu, H.-L., & Roble, R. G. 2008, *Journal of Geophysical Research (Planets)*, 113, 5008
- Tsuchiya, T., Jun, T., Kiochiro, U., & Renata, M., W. 2004, *Earth Planet. Sci. Lett.*, 224, 241
- Uchida, T., Wang, Y., Rivers, M. L., & Sutton, S. R. 2001, *J. Geophys. Res.*, 106, 21799
- Valencia, D., O’Connell, R. J., & Sasselov, D. D. 2006, *Icarus*, 181, 545
- Valencia, D., Sasselov, D. D., & O’Connell, R. J. 2007a, *ApJ*, 656, 545
- Valencia, D., Sasselov, D. D., & O’Connell, R. J. 2007b, *ApJ*, 665, 1413
- Verner, D. A., Ferland, G. J., Korista, K. T., & Yakovlev, D. G. 1996, *ApJ*, 465, 487
- Vidal-Madjar, A., Lecavelier des Etangs, A., Désert, J.-M., Ballester, G. E., Ferlet, R., Hébrard, G., & Mayor, M. 2003, *Nature*, 422, 143
- Vidal-Madjar, A., et al. 2004, *ApJ*, 604, L69
- Wagner, W., Pruff, A. 2002, *J. Phys. Chem. Ref. Data*, 31, 387
- Watson, A. J., Donahue, T. M., & Walker, J. C. G. 1981, *Icarus*, 48, 150
- Wu, Y., & Murray, N. 2003, *ApJ*, 589, 605
- Yelle, R., Lammer, H., & Ip, W.-H. 2008, *Space Science Reviews*, 139, 437